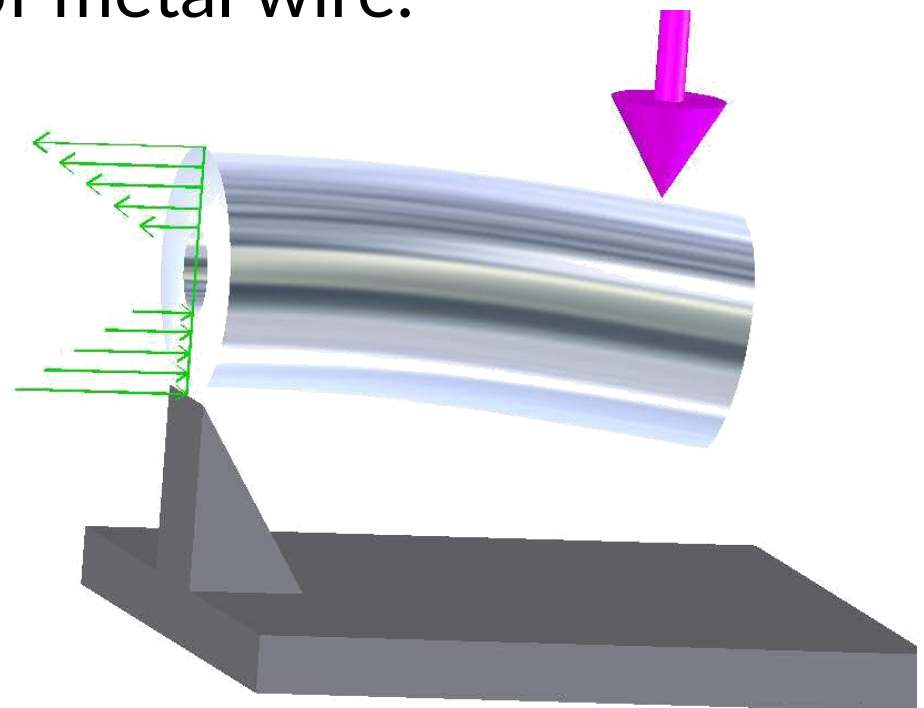


Fatigue failure

Metal fatigue can cause catastrophic failures without warning, such as a fan blade separating from a jet engine, causing damage or even death.

Stress can be applied in different ways. For example, tension stress develops on the outer radius of a bent piece of metal wire.

At the same time, compression stress occurs at the inner radius of the bend. Reversing the bend reverses the compression and tension stresses.



Fatigue failure

When repeated over and over, stress concentrations like these will cause microcracks.

If the stresses continue, the cracks will grow. And because the cracks are small, there may be little or no visible warning.

The result can be an unpredictable metal fatigue failure.

Stresses that Cause Metal Fatigue

In addition to bending, or radial stresses, other types of stresses can cause metal fatigue.

There may be a defect caused by the manufacturing process or within the material itself.

Increased metal fatigue also can occur due to corrosion, part rotation, temperature, wear, or structural design.

For example, the edges of holes tend to concentrate stress, but the hole could be placed elsewhere making the part less susceptible to fatigue.

Stresses that Cause Metal Fatigue

The stresses that cause metal fatigue are usually lower than the material's ultimate tensile strength, and quite frequently even below the yield strength.

Engineers designing a part must understand how much repeated stress the part can handle, and that partly depends on the fatigue strength of the metal.

Forms of Material Fatigue Failure

Metal fatigue failure can be reflected in different forms of fatigue, including:

- **Thermal fatigue failure.** This type of metal fatigue occurs due to temperature changes. These changes can be caused by environmental factors as well as temperature fluctuations from applications being turned off and on.
- **Corrosion fatigue failure.** Commonly due to corrosive environments that damage the metal. Corrosion can initially cause cracks which can cause mechanical damage and fatigue.

Forms of Material Fatigue Failure

- **Vibration fatigue failure.** As the name implies, vibration fatigue is due to vibrational damage that leads to cracks and stresses when equipment is functioning at levels that are out of operational standards.
- **Mechanical failure.** This type of metal fatigue is due to stresses occurring over time and includes corrosion and vibration fatigue failure.

Design Considerations for Determining Metal Fatigue Strength

Different materials have different fatigue strengths. To determine the fatigue strength of a material, engineers will test multiple identical specimens under different cyclic loads until they break.

Many such data points can then be plotted on a graph to determine the fatigue limit of the material.

Using this known value, structural engineers can perform a software fatigue analysis of a part design.

Design Considerations for Determining Metal Fatigue Strength

If needed, they can redesign the part to minimize internal stresses. Or they could specify a different material that would be more resistant to fatigue stress.

Engineering designs where metal fatigue from repeated stresses can cause problems include:

- Jet engine turbofans with rotating propellers
- Airplane body parts
- Off-road bikes
- Bridges with traffic and wind vibration
- Automotive suspensions
- Manufacturing equipment
- Any component under vibrational stress

Aviation Metal Fatigue

Metal fatigue in aircraft is a common occurrence due to the cyclical nature of pressure and stress on aircraft parts and components.

Over time small cracks can increase in size and scope, where metal fatigue can become a contributing factor to mechanical and structural failure.



Aviation Metal Fatigue

Pressure, atmospheric exposure, and general flight conditions can weaken aluminum, carbon steel, and stainless steel aircraft components.

Main areas where metal fatigue occurs in aircraft:

- External areas such as skins that function under structural pressure
- Internal areas where load-bearing components are subjected to high stress environments

Routine maintenance and inspection can help offset aviation metal fatigue while polishing the aircraft's metal surfaces can also help slow the effects of cracks and fatigue.

Fatigue failure

Often, machine members are found to have failed under the action of repeated or fluctuating stresses; yet the most careful analysis reveals that the actual maximum stresses were well below the ultimate strength of the material, and quite frequently even **below the yield strength**.

The most distinguishing characteristic of these failures is that the stresses have been repeated a very large number of times.

Hence the failure is called a *fatigue failure*.

Fatigue failure

When machine parts fail statically, they usually develop a very large deflection, because the stress has exceeded the yield strength, and the part is replaced before fracture actually occurs.

Thus many static failures give visible warning in advance.

But a fatigue failure gives no warning! It is **sudden** and **total**, and hence **dangerous**.

Fatigue failure

Aloha airlines flight 243 April 28th 1988
Metal Fatigue!



Fatigue failure

Date	Accident/incident	location	Aircraft	cause	Fatalities	Notes
1997-06-26	Helikopter Service Flight 451	Norway: Norwegian Sea	Eurocopter AS 332L1 Super Puma	Fatigue	12	The accident was caused by a fatigue crack in the spline , which ultimately caused the power transmission shaft to fail. The helicopter crashed into the sea
1976-04-14	Yacimientos Petroliferos Fiscales	Argentina : near Cutral-Co	Hawker Siddeley 748	maintenance: undetected metal fatigue	34	starboard wing failed outboard of engine
1978-06-26	Helikopter Service Flight 165	Norway: North Sea	Sikorsky S-61	Fatigue	18	rotor blade loosened after fatigue to the knuckle joint : crashed into the sea

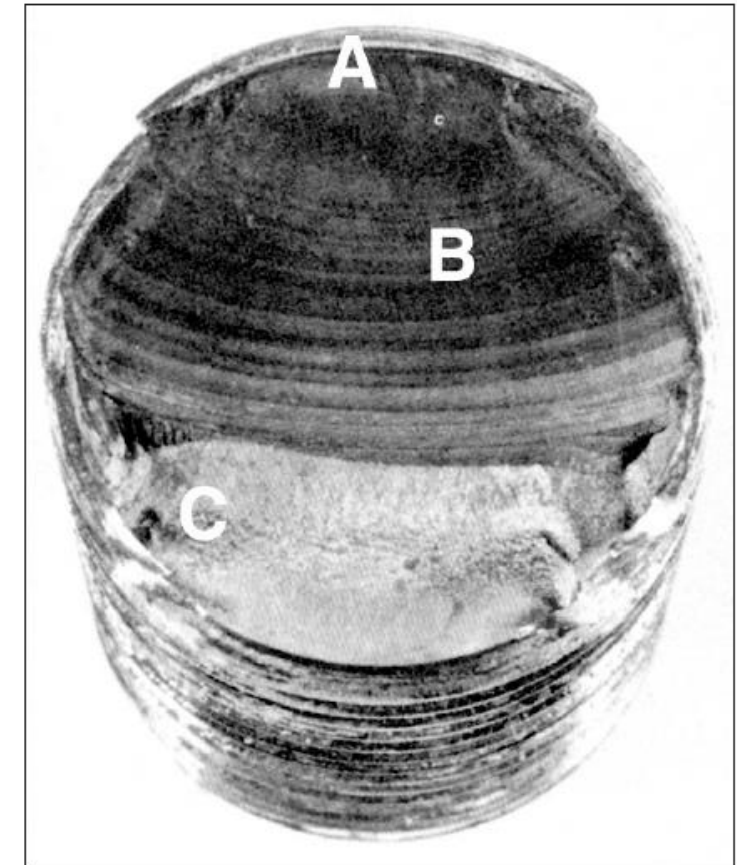
Fatigue failure

A fatigue failure has an appearance similar to a brittle fracture, as the fracture surfaces are flat and perpendicular to the stress axis with the absence of necking.

It has three stages of development:

Stage I (A) is the initiation of one or more micro-cracks due to cyclic plastic deformation followed by crystallographic propagation extending from two to five grains about the origin.

Stage I cracks are not normally visible to the naked eye

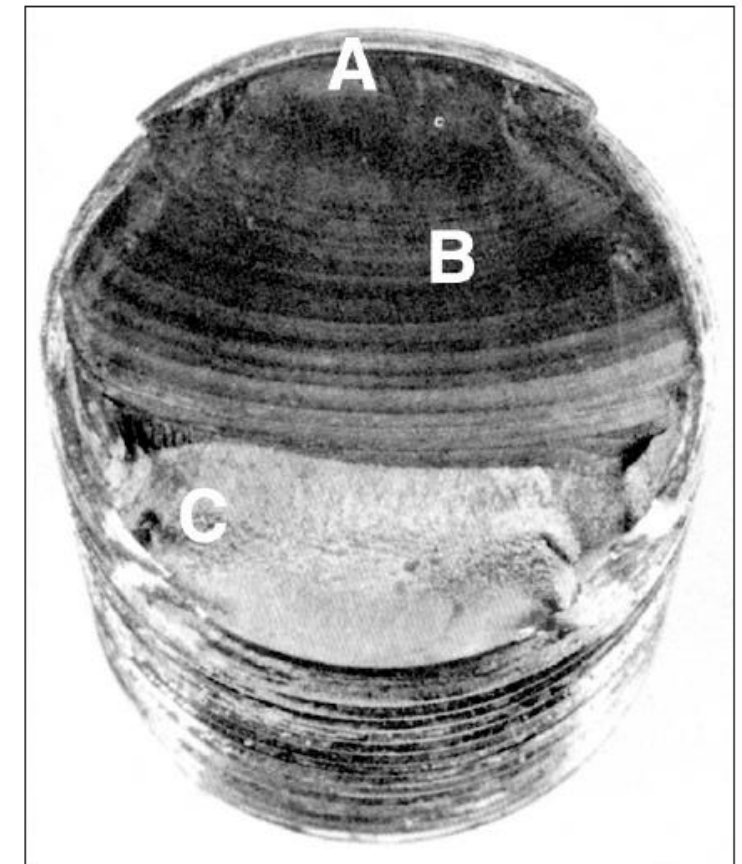


Fatigue failure

Stage II (B) progresses from micro-cracks to macro-cracks forming parallel plateau-like fracture surfaces separated by longitudinal ridges.

The plateaus are generally smooth and normal to the direction of maximum tensile stress.

These surfaces can be wavy dark and light bands referred to as *beach marks*.

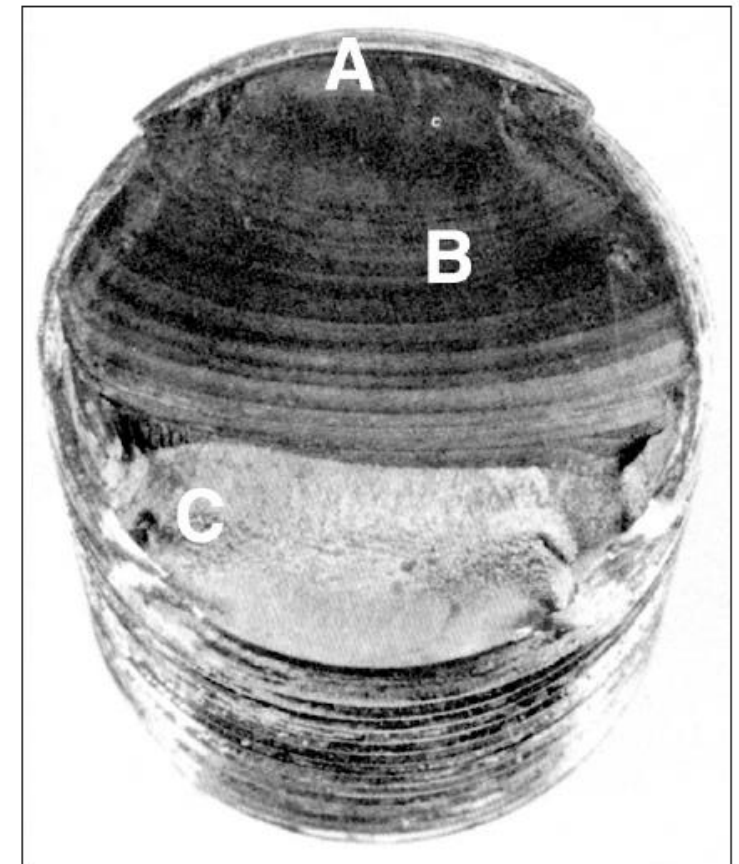


Fatigue failure

Stage III (c) occurs during the final stress cycle when the remaining material cannot support the loads, resulting in a sudden, fast fracture.

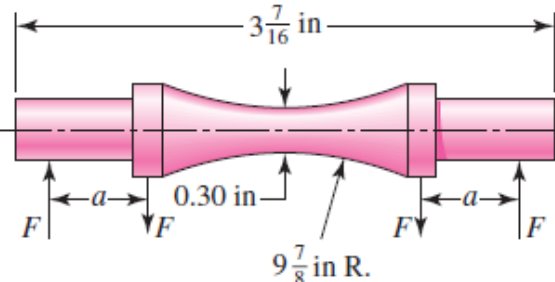
A stage III fracture can be brittle, ductile, or a combination of both.

Quite often the beach marks, if they exist, and possible patterns in the stage III fracture called *chevron lines*, point toward the origins of the initial cracks.

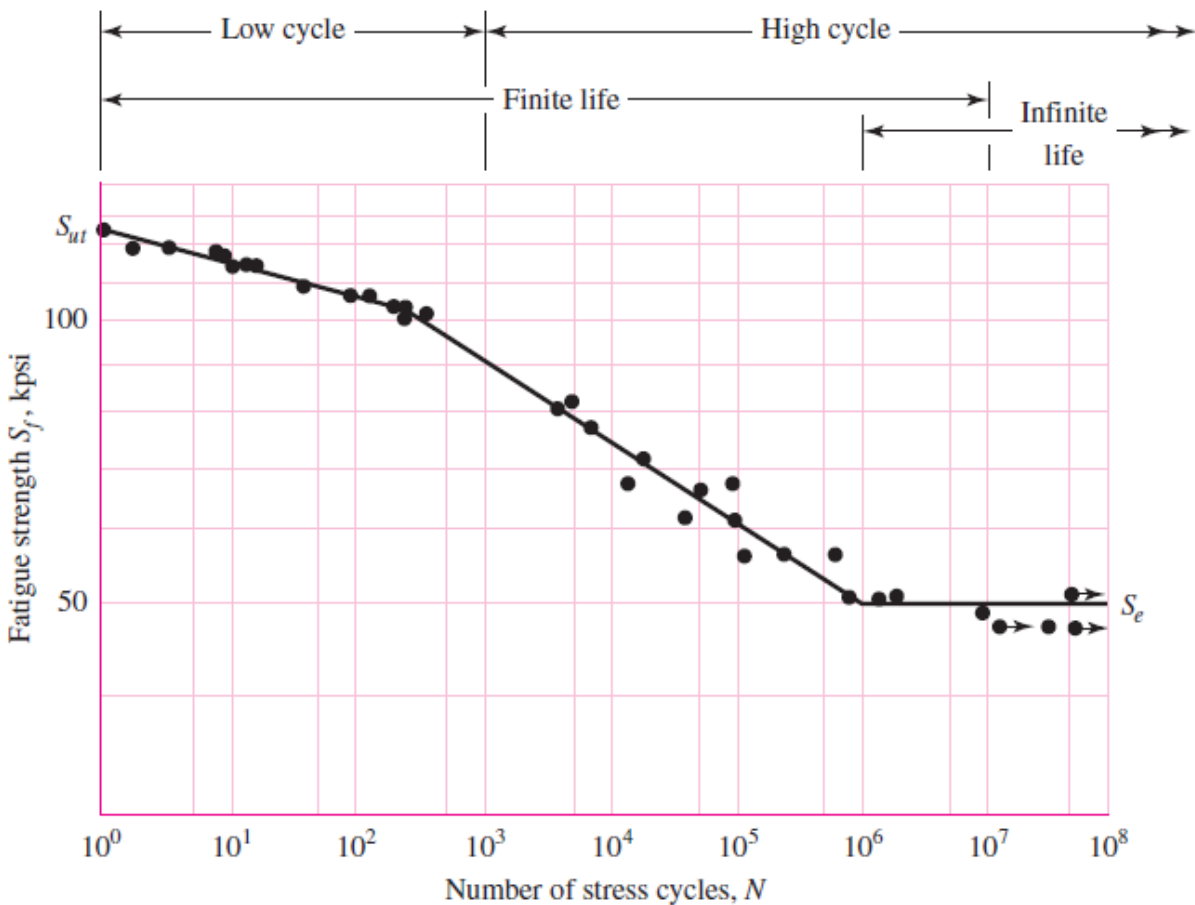


Fatigue Analysis

Test-specimen geometry for the R. R. Moore rotating-beam machine. The bending moment is uniform, $M = Fa$, over the curved length and at the highest-stressed section at the mid-point of the beam.



An $S-N$ diagram plotted from the results of completely reversed axial fatigue tests. Material: UNS G41300 steel, normalized; $S_{ut} = 116$ kpsi; maximum $S_{ut} = 125$ kpsi.
(Data from NACA Tech. Note 3866, December 1966.)

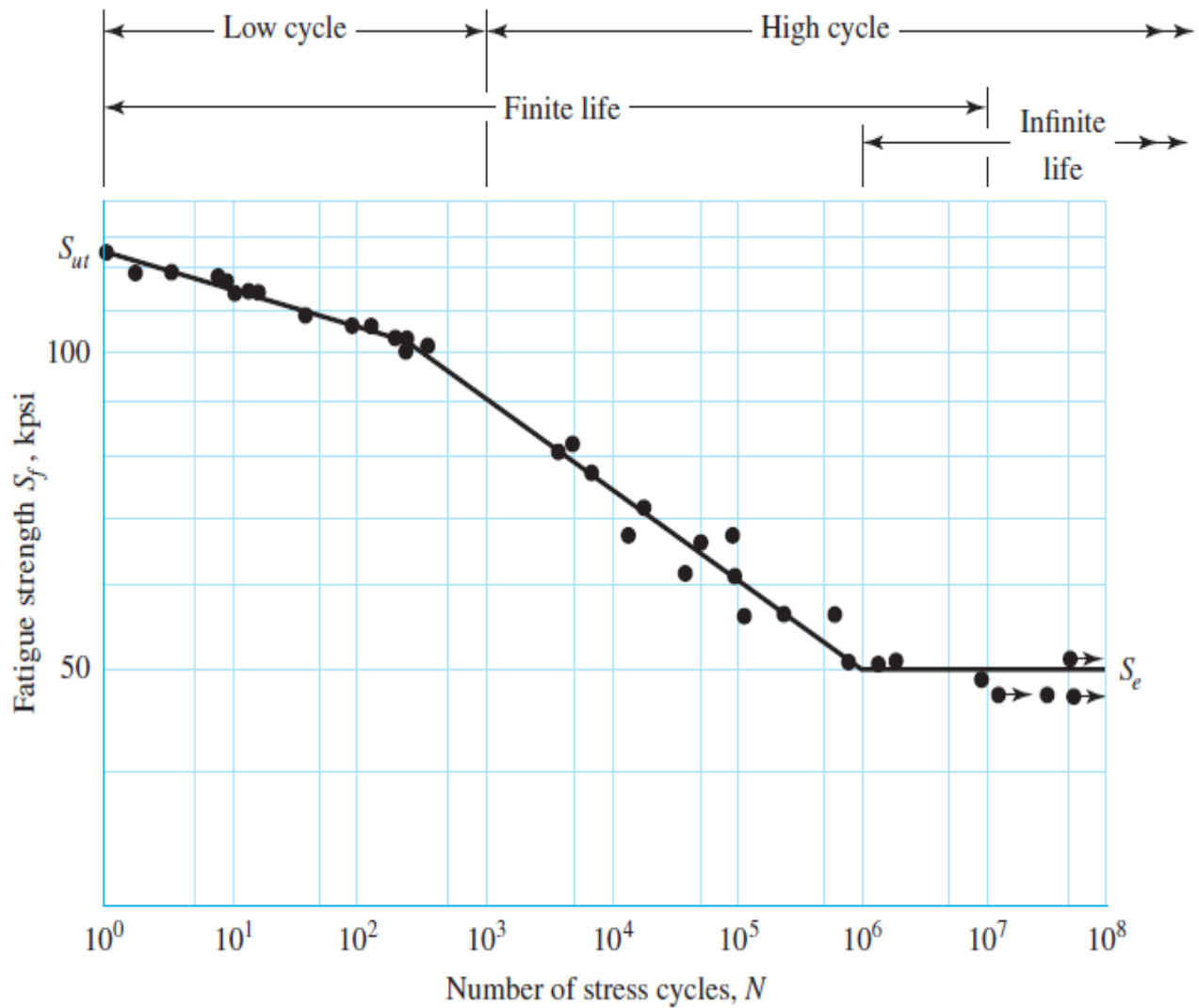


Fatigue Strength

Region of low-cycle fatigue extends from $N = 1$ to about 10^3 cycles.

In this region the fatigue strength S_f is only slightly smaller than the tensile strength S_{ut} .

high-cycle fatigue domain extends from 10^3 cycles for steels to the endurance limit life N_e , which is about 10^6 to 10^7 cycles.



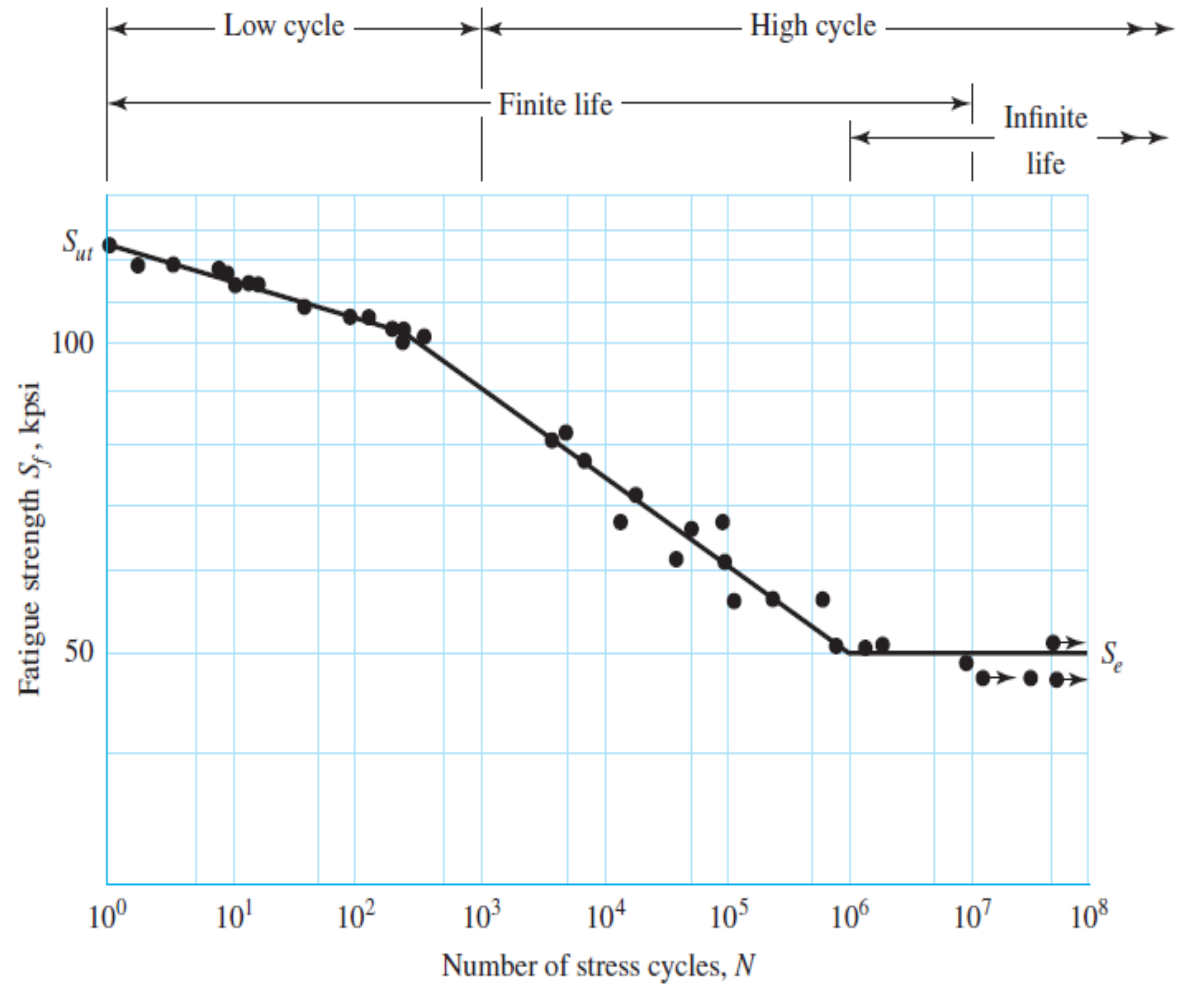
Fatigue Strength

Experience has shown high-cycle fatigue data are rectified by a logarithmic transform to both stress and cycles-to-failure.

$$S_f = a N^b$$

$$a = \frac{(f S_{ut})^2}{S_e}$$

$$b = -\frac{1}{3} \log \left(\frac{f S_{ut}}{S_e} \right)$$



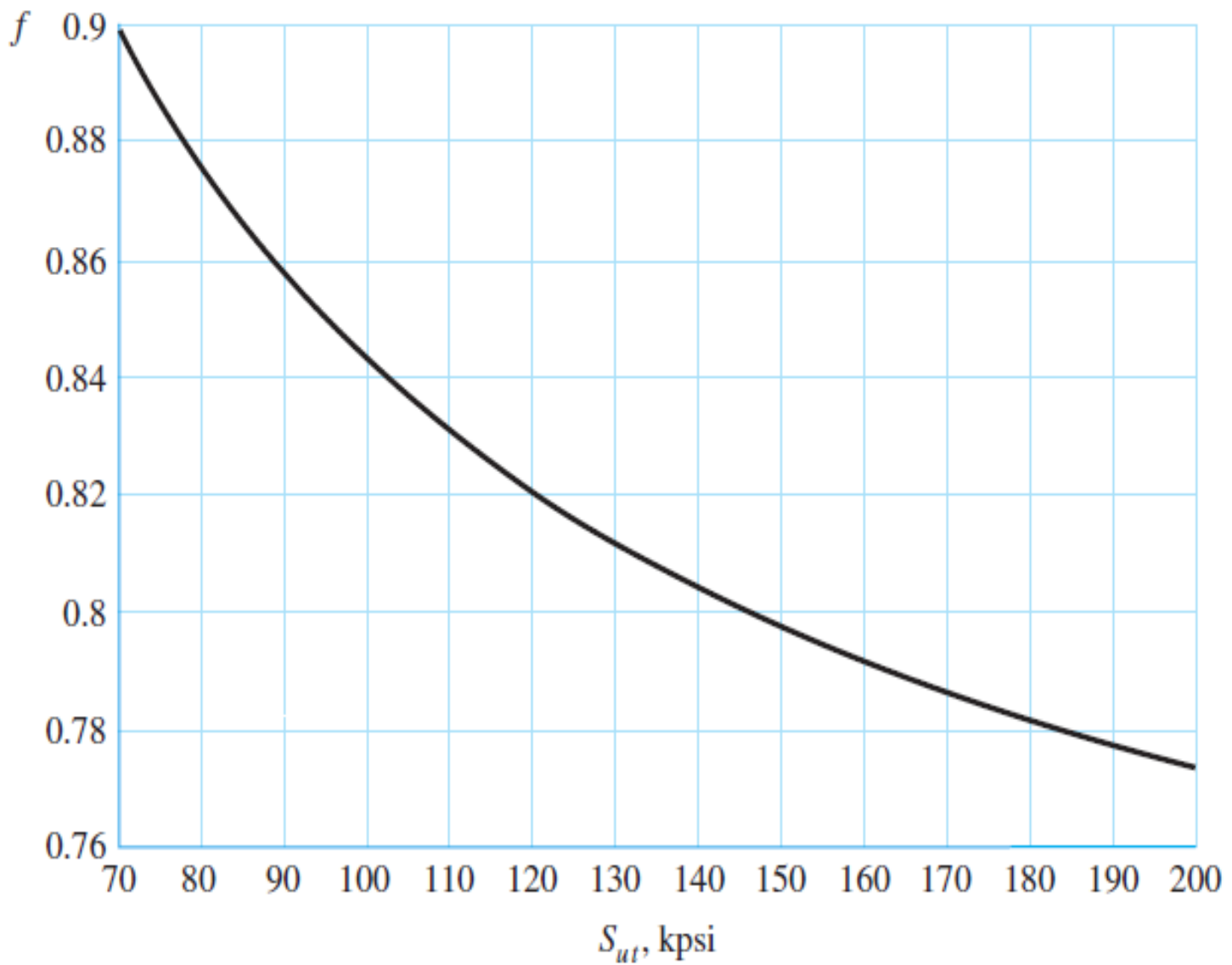
Fatigue Strength

$$S_f = a N^b$$

$$a = \frac{(f S_{ut})^2}{S_e}$$

$$b = -\frac{1}{3} \log \left(\frac{f S_{ut}}{S_e} \right)$$

where f is the fraction of S_{ut} represented by $(S'_f) 10^3$ cycles.

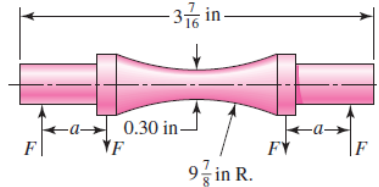


Fatigue Analysis

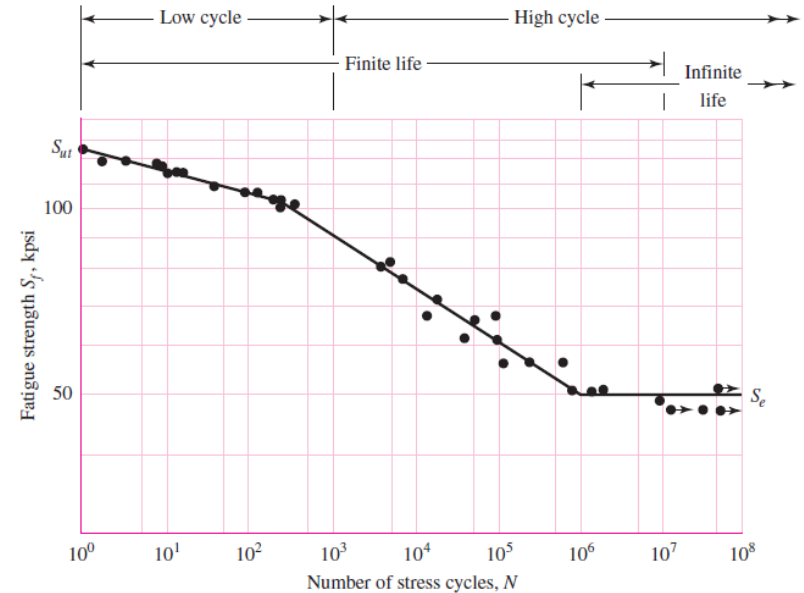
In the case of the steels, a knee occurs in the graph, and beyond this knee failure will not occur, no matter how great the number of cycles.

The strength corresponding to the knee is called the **endurance limit S_e** , or the fatigue limit.

Test-specimen geometry for the R. R. Moore rotating-beam machine. The bending moment is uniform, $M = Fa$, over the curved length and at the highest-stressed section at the mid-point of the beam.



An $S-N$ diagram plotted from the results of completely reversed axial fatigue tests. Material: UNS G41300 steel, normalized; $S_{ut} = 116$ kpsi; maximum $S_{ut} = 125$ kpsi. (Data from NACA Tech. Note 3866, December 1966.)



$$S'_e = \begin{cases} 0.5S_{ut} & S_{ut} \leq 200 \text{ kpsi (1400 MPa)} \\ 100 \text{ kpsi} & S_{ut} > 200 \text{ kpsi} \\ 700 \text{ MPa} & S_{ut} > 1400 \text{ MPa} \end{cases}$$

Fatigue Analysis

$$S_e = k_a k_b k_c k_d k_e k_f S'_e$$

where k_a = surface condition modification factor
 k_b = size modification factor
 k_c = load modification factor
 k_d = temperature modification factor
 k_e = reliability factor¹³
 k_f = miscellaneous-effects modification factor
 S'_e = rotary-beam test specimen endurance limit
 S_e = endurance limit at the critical location of a machine part in the geometry and condition of use

Fatigue Analysis

Surface Factor

The surface of a rotating-beam specimen is highly polished, with a final polishing in the axial direction to smooth out any circumferential scratches.

The surface modification factor depends on the quality of the finish of the actual part surface and on the tensile strength of the part material.

$$k_a = a S_{ut}^b$$

where S_{ut} is the minimum tensile strength and a and b are to be found in Table 6-2.

Fatigue Analysis

Surface Finish	S_{ut}, kpsi	Factor a	S_{ut}, MPa	Exponent b
Ground	1.34		1.58	-0.085
Machined or cold-drawn	2.70		4.51	-0.265
Hot-rolled	14.4		57.7	-0.718
As-forged	39.9		272.	-0.995

Fatigue Analysis

Size Factor

$$k_b = \begin{cases} (d/0.3)^{-0.107} = 0.879d^{-0.107} & 0.11 \leq d \leq 2 \text{ in} \\ 0.91d^{-0.157} & 2 < d \leq 10 \text{ in} \\ (d/7.62)^{-0.107} = 1.24d^{-0.107} & 2.79 \leq d \leq 51 \text{ mm} \\ 1.51d^{-0.157} & 51 < d \leq 254 \text{ mm} \end{cases}$$

For axial loading there is no size effect, so

$$k_b = 1$$

but see k_c .

Fatigue Analysis

Size Factor

One of the problems that arises in using the equation for the size factor is what to do when a round bar in bending is not rotating, or when a noncircular cross section is used. For example, what is the size factor for a bar 6 mm thick and 40 mm wide?

We use an *equivalent diameter* d_e obtained by equating the volume of material stressed at and above 95 percent of the maximum stress to the same volume in the rotating-beam specimen

Fatigue Analysis

Size Factor

For a rotating round section $A_{0.95\sigma} = \frac{\pi}{4} [d^2 - (0.95d)^2] = 0.0766d^2$

For nonrotating solid or hollow Rounds $d_e = 0.370d$

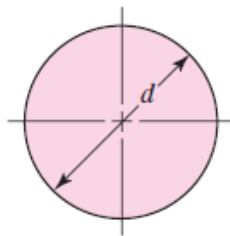
$$A_{0.95\sigma} = 0.01046d^2$$

A rectangular section of dimensions $h \times b$ has $d_e = 0.808(hb)^{1/2}$

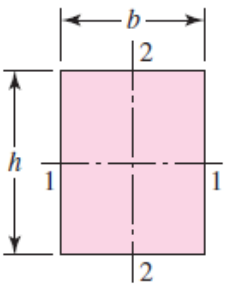
$$A_{0.95\sigma} = 0.05hb$$

Fatigue Analysis

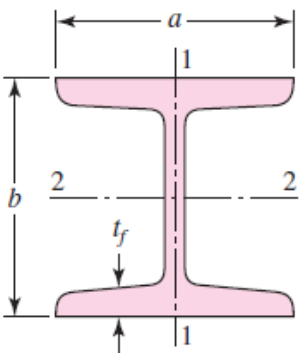
Size Factor



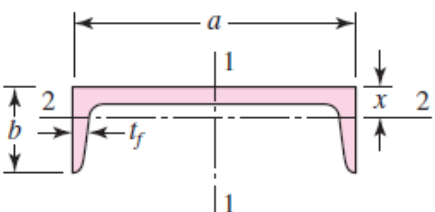
$$A_{0.95\sigma} = 0.01046d^2$$
$$d_e = 0.370d$$



$$A_{0.95\sigma} = 0.05hb$$
$$d_e = 0.808\sqrt{hb}$$



$$A_{0.95\sigma} = \begin{cases} 0.10at_f & \text{axis 1-1} \\ 0.05ba & \text{axis 2-2} \\ t_f > 0.025a \end{cases}$$



$$A_{0.95\sigma} = \begin{cases} 0.05ab & \text{axis 1-1} \\ 0.052xa + 0.1t_f(b-x) & \text{axis 2-2} \end{cases}$$

Fatigue Analysis

Loading Factor

$$k_c = \begin{cases} 1 & \text{bending} \\ 0.85 & \text{axial} \\ 0.59 & \text{torsion}^{17} \end{cases}$$

¹⁷Use this only for pure torsional fatigue loading. When torsion is combined with other stresses, such as bending, $k_c = 1$ and the combined loading is managed by using the effective von Mises stress as in Sec. 5–5.
Note: For pure torsion, the distortion energy predicts that $(k_c)_{\text{torsion}} = 0.577$.

Fatigue Analysis

Temperature Factor

When operating temperatures are below room temperature, brittle fracture is a strong possibility and should be investigated first.

$$k_d = 0.975 + 0.432(10^{-3})T_F - 0.115(10^{-5})T_F^2 \\ + 0.104(10^{-8})T_F^3 - 0.595(10^{-12})T_F^4$$

where $70 \leq T_F \leq 1000^{\circ}\text{F}$.

When the operating temperatures are higher than room temperature, yielding should be investigated first because the yield strength drops off so rapidly with temperature. Or use

$$k_d = \frac{S_T}{S_{RT}}$$

Fatigue Analysis

Temperature Factor

Temperature, °C	S_T/S_{RT}	Temperature, °F	S_T/S_{RT}
20	1.000	70	1.000
50	1.010	100	1.008
100	1.020	200	1.020
150	1.025	300	1.024
200	1.020	400	1.018
250	1.000	500	0.995
300	0.975	600	0.963
350	0.943	700	0.927
400	0.900	800	0.872
450	0.843	900	0.797
500	0.768	1000	0.698
550	0.672	1100	0.567
600	0.549		

Fatigue Analysis

Reliability Factor

Reliability, %	Transformation Variate z_a	Reliability Factor k_e
50	0	1.000
90	1.288	0.897
95	1.645	0.868
99	2.326	0.814
99.9	3.091	0.753
99.99	3.719	0.702
99.999	4.265	0.659
99.9999	4.753	0.620

Fatigue Analysis

Miscellaneous-Effects Factor

Though the factor k_f is intended to account for the reduction in endurance limit due to all other effects, it is really intended as a reminder that these must be accounted for, because actual values of k_f are not always available.

Residual stresses

Corrosion

Electrolytic Plating

Metal Spraying

Cyclic Frequency

Fretting (wear) Corrosion

Stress Concentration and Notch Sensitivity

The existence of irregularities or discontinuities, such as holes, grooves, or notches, in a part increases the theoretical stresses significantly in the immediate vicinity of the discontinuity.

Stress concentration factor K_t (or K_{ts}), is thus to be used with the nominal stress to obtain the maximum resulting stress due to the irregularity or defect.

Figure A-15-15

Grooved round bar in torsion.
 $\tau_0 = Tc/J$, where $c = d/2$ and
 $J = \pi d^4/32$.

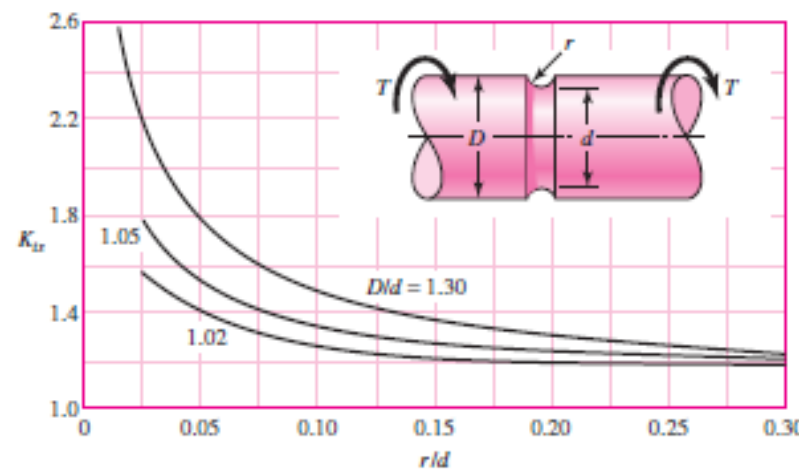
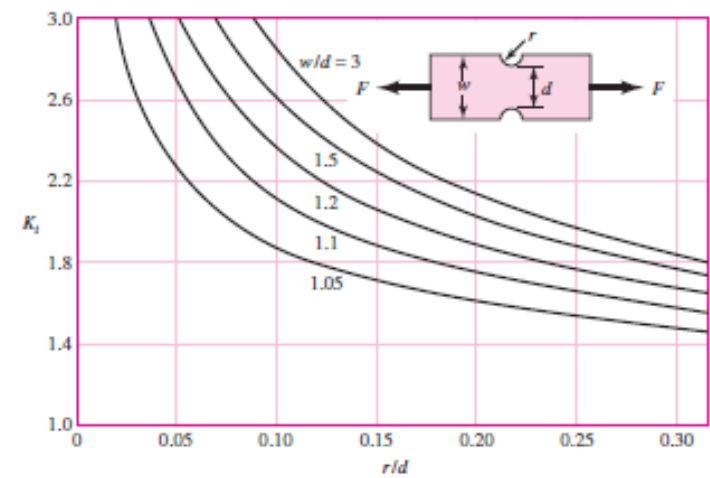


Figure A-15-3

Notched rectangular bar in tension or simple compression.
 $\sigma_0 = F/A$, where $A = dt$ and t is the thickness.



Stress Concentration and Notch Sensitivity

It turns out that some materials are not fully sensitive to the presence of notches and hence, for these, a reduced value of K_t can be used. For these materials, the effective maximum stress in fatigue is:

$$\sigma_{max} = K_f \sigma_0 \text{ or } \tau_{max} = K_{fs} \tau_0$$

where K_f is a reduced value of K_t and σ_0 is the nominal stress. The factor K_f is commonly called a *fatigue stress-concentration factor*, and hence the subscript f.

$$K_f = \frac{\text{maximum stress in notched specimen}}{\text{stress in notch-free specimen}}$$

Stress Concentration and Notch Sensitivity

Notch sensitivity q is defined by the equation

$$q = \frac{K_f - 1}{K_t - 1} \quad \text{or} \quad q_{\text{shear}} = \frac{K_{fs} - 1}{K_{ts} - 1}$$

where q is usually between zero and unity.

The equation shows that if $q = 0$, then $K_f = 1$, and the material has no sensitivity to notches at all.

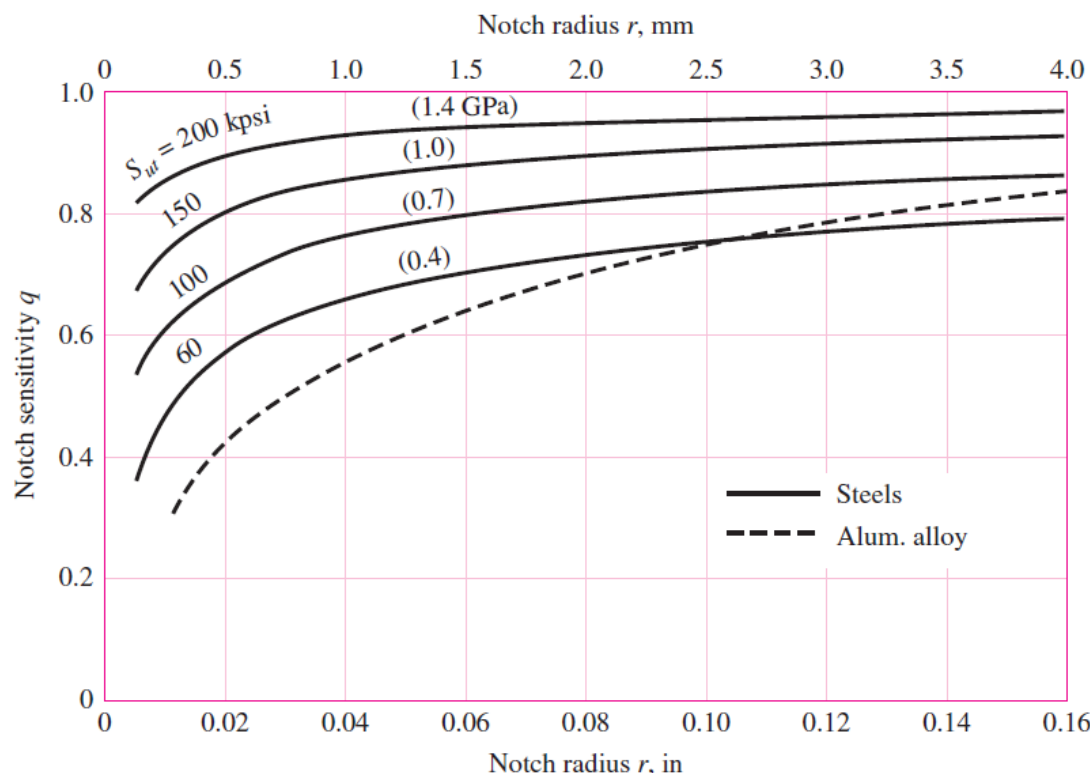
On the other hand, if $q = 1$, then $K_f = K_t$, and the material has full notch sensitivity.

Stress Concentration and Notch Sensitivity

In analysis or design work, find K_t first, from the geometry of the part. Then specify the material, find q , and solve for K_f from the equation $K_f = 1 + q(K_t - 1)$ or $K_{fs} = 1 + q_{shear}(K_{ts} - 1)$

Figure 6-20

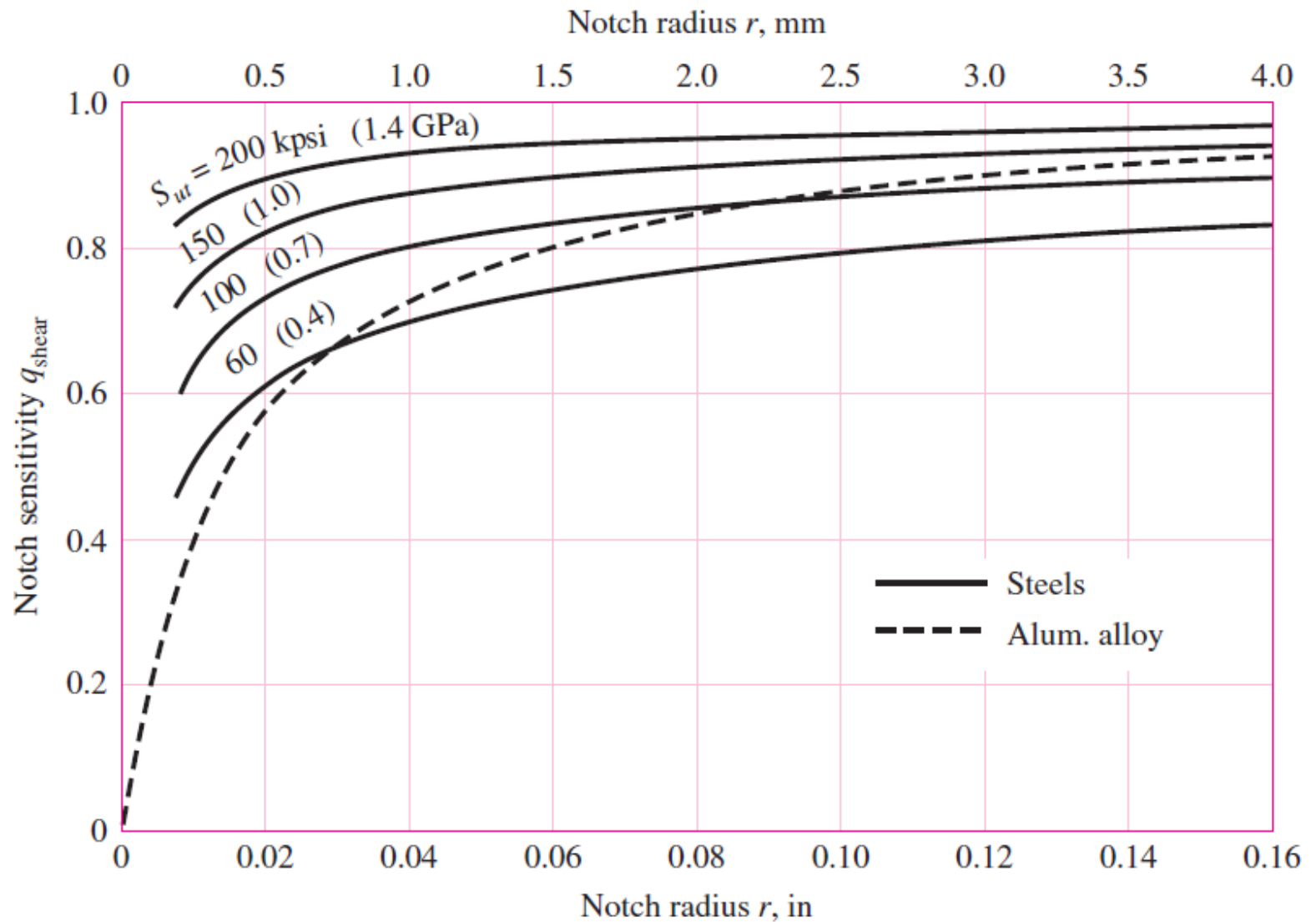
Notch-sensitivity charts for steels and UNS A92024-T wrought aluminum alloys subjected to reversed bending or reversed axial loads. For larger notch radii, use the values of q corresponding to the $r = 0.16$ -in (4-mm) ordinate. (From George Sines and J. L. Waisman (eds.), Metal Fatigue, McGraw-Hill, New York. Copyright © 1969 by The McGraw-Hill Companies, Inc. Reprinted by permission.)



Stress Concentration and Notch Sensitivity

Figure 6-21

Notch-sensitivity curves for materials in reversed torsion. For larger notch radii, use the values of q_{shear} corresponding to $r = 0.16$ in (4 mm).



Stress Concentration and Notch Sensitivity

The Figure has as its basis the *Neuber equation*, which is given by

$$q = \frac{1}{1 + \frac{\sqrt{a}}{\sqrt{r}}}$$

Where \sqrt{a} is defined as the *Neuber constant* and is a material constant.

Bending or axial: $\sqrt{a} = 0.246 - 3.08(10^{-3})S_{ut} + 1.51(10^{-5})S_{ut}^2 - 2.67(10^{-8})S_{ut}^3$

Torsion: $\sqrt{a} = 0.190 - 2.51(10^{-3})S_{ut} + 1.35(10^{-5})S_{ut}^2 - 2.67(10^{-8})S_{ut}^3$

Characterizing Fluctuating Stresses

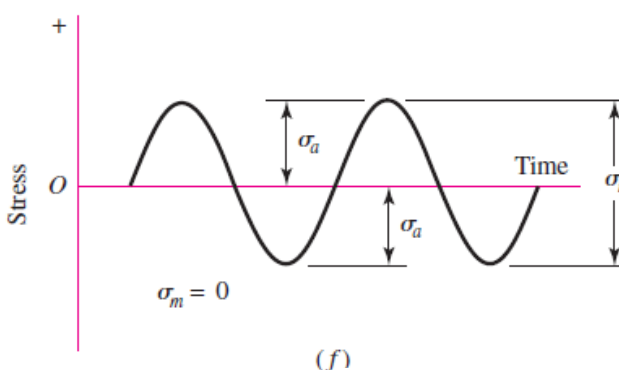
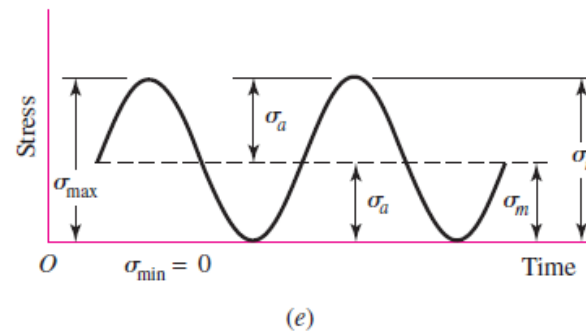
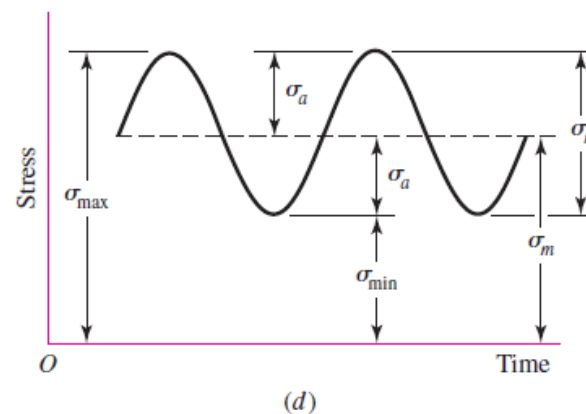
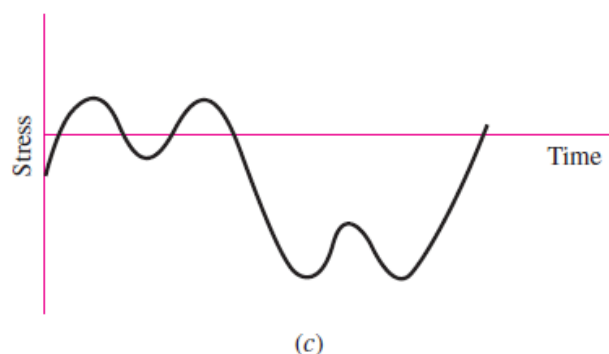
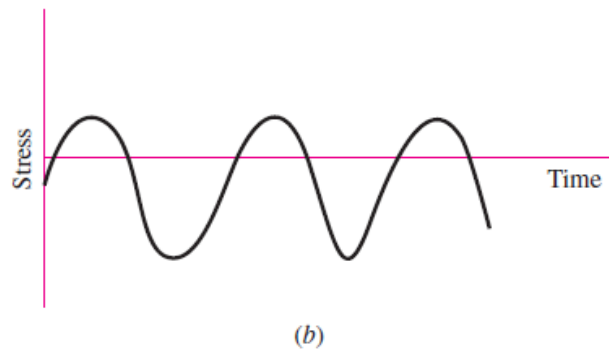
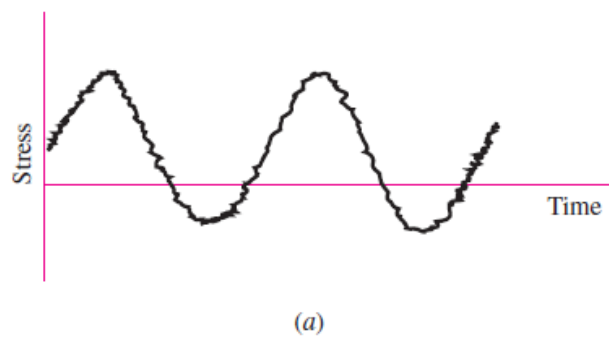
Fluctuating stresses in machinery often take the form of a sinusoidal pattern because of the nature of some rotating machinery. However, other patterns, some quite irregular, do occur.

$$F_m = \frac{F_{\max} + F_{\min}}{2} \quad F_a = \left| \frac{F_{\max} - F_{\min}}{2} \right|$$

where F_m is midrange steady component of force, and F_a is the amplitude of the alternating component the of force.

Figure 6-23

Some stress-time relations:
(a) fluctuating stress with high-frequency ripple; (b and c) nonsinusoidal fluctuating stress; (d) sinusoidal fluctuating stress; (e) repeated stress; (f) completely reversed sinusoidal stress.



σ_{min} = minimum stress

σ_{max} = maximum stress

σ_a = amplitude component

σ_m = midrange component

σ_r = range of stress

σ_s = static or steady stress

Characterizing Fluctuating Stresses

The following relations are evident

$$F_m = \frac{F_{\max} + F_{\min}}{2}$$

$$F_a = \left| \frac{F_{\max} - F_{\min}}{2} \right|$$

$$\sigma_m = \frac{\sigma_{\max} + \sigma_{\min}}{2}$$

$$\sigma_a = \left| \frac{\sigma_{\max} - \sigma_{\min}}{2} \right|$$

In addition, the *stress ratio*

$$R = \frac{\sigma_{\min}}{\sigma_{\max}}$$

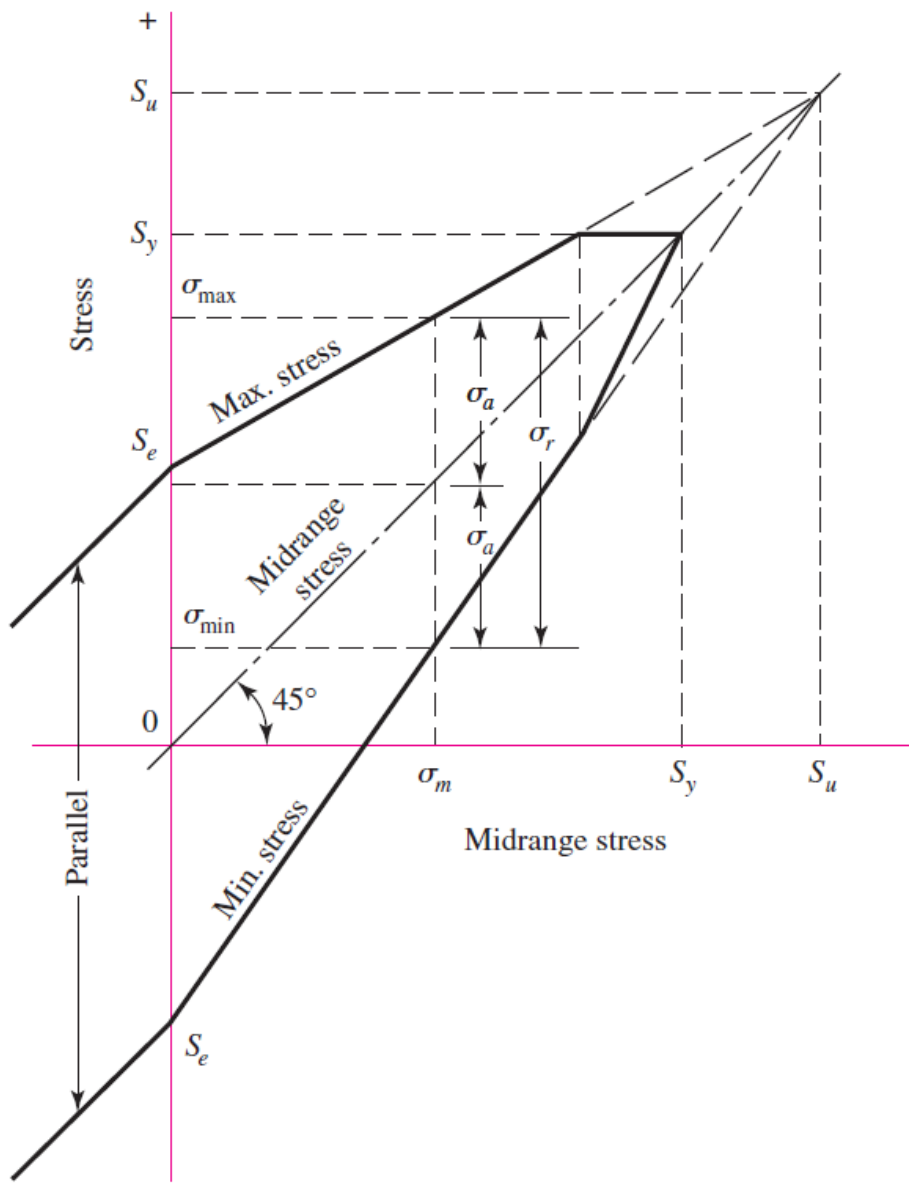
and the *amplitude ratio*

$$A = \frac{\sigma_a}{\sigma_m}$$

Fatigue Failure Criteria for Fluctuating Stress

Figure 6-24

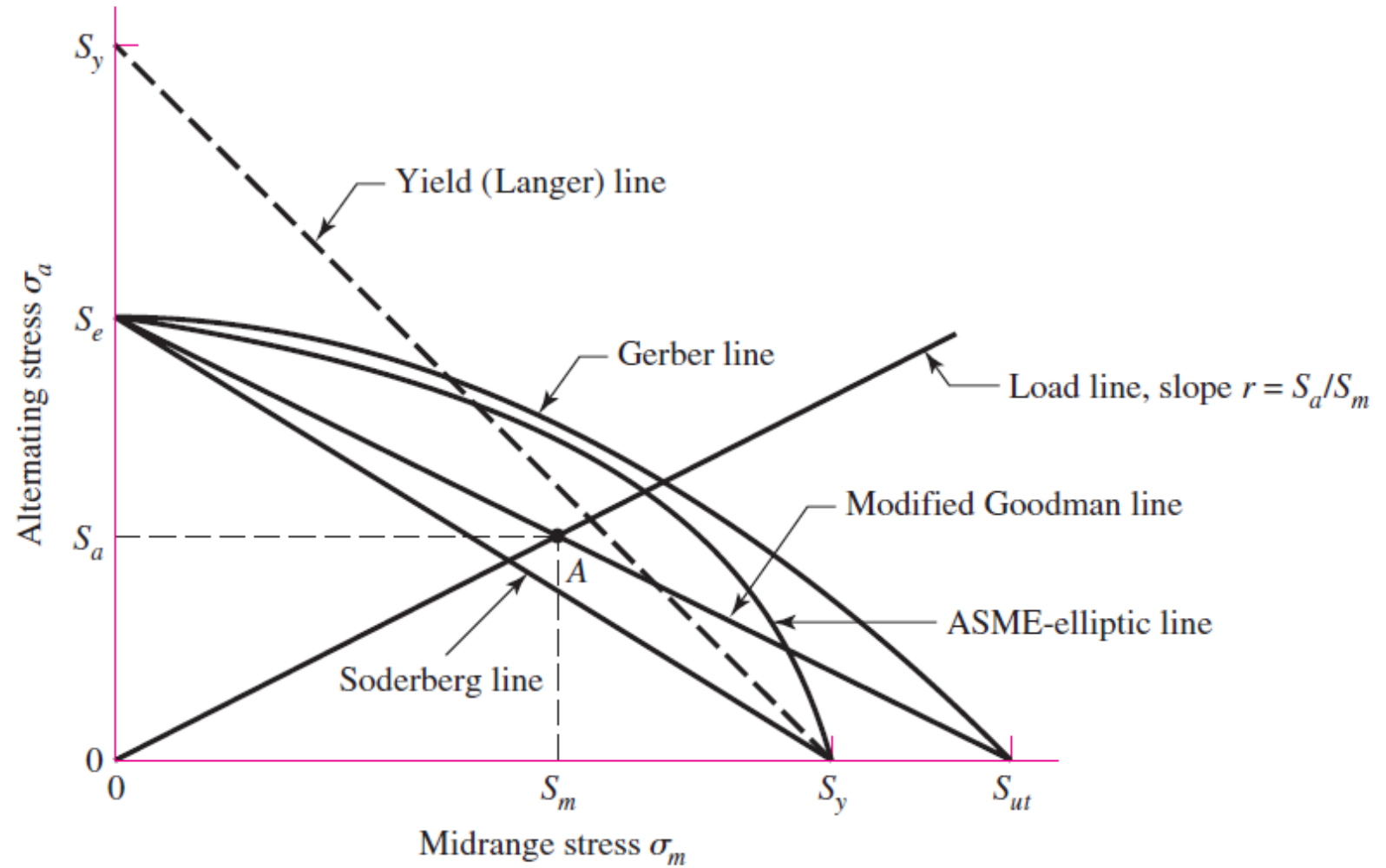
Modified Goodman diagram showing all the strengths and the limiting values of all the stress components for a particular midrange stress.



Fatigue Failure Criteria for Fluctuating Stress

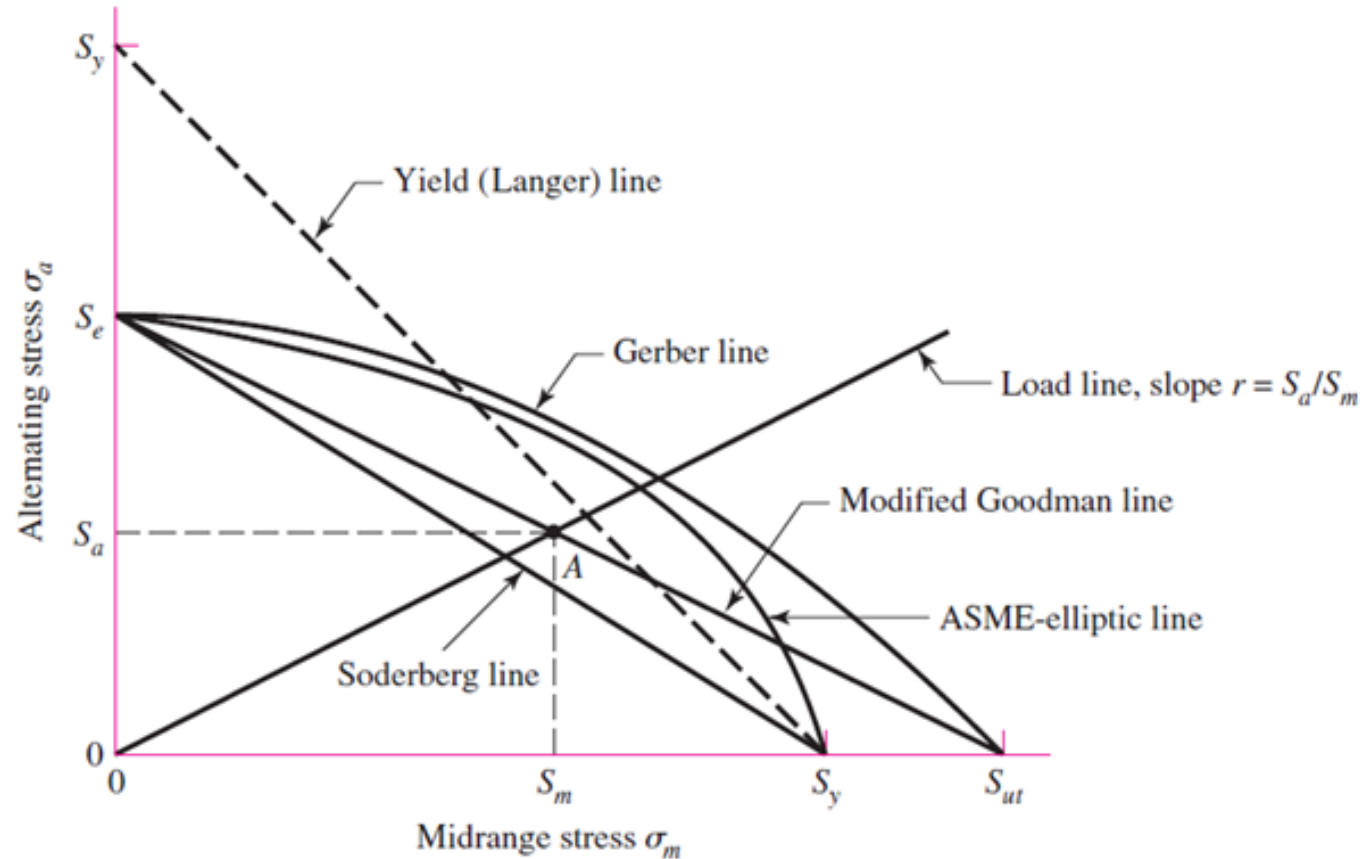
Figure 6-27

Fatigue diagram showing various criteria of failure. For each criterion, points on or “above” the respective line indicate failure. Some point A on the Goodman line, for example, gives the strength S_m as the limiting value of σ_m corresponding to the strength S_a , which, paired with σ_m , is the limiting value of σ_a .



Fatigue Failure Criteria for Fluctuating Stress

Five criteria of failure are diagrammed: the **Soderberg**, the **modified Goodman**, the **Gerber**, the **ASME-elliptic**, and **yielding**.



The diagram shows that only the Soderberg criterion guards against any yielding, but is biased low.

Fatigue Failure Criteria for Fluctuating Stress

Considering the modified Goodman line as a criterion, point *A* represents a limiting point with an alternating strength S_a and midrange strength S_m . The slope of the load line shown is defined as $r = S_a/S_m$.

The criterion equation for the Soderberg line is

$$\frac{S_a}{S_e} + \frac{S_m}{S_y} = 1$$

Similarly, we find the modified Goodman relation to be

$$\frac{S_a}{S_e} + \frac{S_m}{S_{ut}} = 1$$

Examination of Fig. 6-25 shows that both a parabola and an ellipse have a better opportunity to pass among the midrange tension data and to permit quantification of the probability of failure. The Gerber failure criterion is written as

$$\frac{S_a}{S_e} + \left(\frac{S_m}{S_{ut}} \right)^2 = 1$$

and the ASME-elliptic is written as

$$\left(\frac{S_a}{S_e} \right)^2 + \left(\frac{S_m}{S_y} \right)^2 = 1$$

Fatigue Failure Criteria for Fluctuating Stress

The *Langer* first-cycle-yielding criterion is used in connection with the fatigue curve:

$$S_a + S_m = S_y$$

The stresses $n\sigma_a$ and $n\sigma_m$ can replace S_a and S_m , where n is the design factor or factor of safety. Then, Eq. (6-40), the Soderberg line, becomes

$$\text{Soderberg} \quad \frac{\sigma_a}{S_e} + \frac{\sigma_m}{S_y} = \frac{1}{n}$$

Equation (6-41), the modified Goodman line, becomes

$$\text{mod-Goodman} \quad \frac{\sigma_a}{S_e} + \frac{\sigma_m}{S_{ut}} = \frac{1}{n}$$

Equation (6-42), the Gerber line, becomes

$$\text{Gerber} \quad \frac{n\sigma_a}{S_e} + \left(\frac{n\sigma_m}{S_{ut}} \right)^2 = 1$$

Equation (6-43), the ASME-elliptic line, becomes

$$\text{ASME-elliptic} \quad \left(\frac{n\sigma_a}{S_e} \right)^2 + \left(\frac{n\sigma_m}{S_y} \right)^2 = 1$$

$$\text{Langer static yield} \quad \sigma_a + \sigma_m = \frac{S_y}{n}$$

Fatigue Failure Criteria for Fluctuating Stress

Table 6-6

Amplitude and Steady
Coordinates of Strength
and Important
Intersections in First
Quadrant for Modified
Goodman and Langer
Failure Criteria

Intersecting Equations	Intersection Coordinates
$\frac{S_a}{S_e} + \frac{S_m}{S_{ut}} = 1$ Load line $r = \frac{S_a}{S_m}$	$S_a = \frac{r S_e S_{ut}}{r S_{ut} + S_e}$ $S_m = \frac{S_a}{r}$
$\frac{S_a}{S_y} + \frac{S_m}{S_y} = 1$ Load line $r = \frac{S_a}{S_m}$	$S_a = \frac{r S_y}{1 + r}$ $S_m = \frac{S_y}{1 + r}$
$\frac{S_a}{S_e} + \frac{S_m}{S_{ut}} = 1$ $\frac{S_a}{S_y} + \frac{S_m}{S_y} = 1$	$S_m = \frac{(S_y - S_e) S_{ut}}{S_{ut} - S_e}$ $S_a = S_y - S_m, r_{crit} = S_a/S_m$

Fatigue factor of safety

$$n_f = \frac{1}{\frac{\sigma_a}{S_e} + \frac{\sigma_m}{S_{ut}}}$$

Fatigue Failure Criteria for Fluctuating Stress

Table 6-7

Amplitude and Steady
Coordinates of Strength
and Importance

Intersections in First
Quadrant for Gerber and
Langer Failure Criteria

Intersecting Equations	Intersection Coordinates
$\frac{S_a}{S_e} + \left(\frac{S_m}{S_{ut}} \right)^2 = 1$	$S_a = \frac{r^2 S_{ut}^2}{2S_e} \left[-1 + \sqrt{1 + \left(\frac{2S_e}{rS_{ut}} \right)^2} \right]$
Load line $r = \frac{S_a}{S_m}$	$S_m = \frac{S_a}{r}$
$\frac{S_a}{S_y} + \frac{S_m}{S_y} = 1$	$S_a = \frac{rS_y}{1+r}$
Load line $r = \frac{S_a}{S_m}$	$S_m = \frac{S_y}{1+r}$
$\frac{S_a}{S_e} + \left(\frac{S_m}{S_{ut}} \right)^2 = 1$	$S_m = \frac{S_{ut}^2}{2S_e} \left[1 - \sqrt{1 + \left(\frac{2S_e}{S_{ut}} \right)^2 \left(1 - \frac{S_y}{S_e} \right)} \right]$
$\frac{S_a}{S_y} + \frac{S_m}{S_y} = 1$	$S_a = S_y - S_m, r_{\text{crit}} = S_a/S_m$
Fatigue factor of safety	
$n_f = \frac{1}{2} \left(\frac{S_{ut}}{\sigma_m} \right)^2 \frac{\sigma_a}{S_e} \left[-1 + \sqrt{1 + \left(\frac{2\sigma_m S_e}{S_{ut} \sigma_a} \right)^2} \right] \quad \sigma_m > 0$	

Fatigue Failure Criteria for Fluctuating Stress

Table 6-8

Amplitude and Steady
Coordinates of Strength
and Importance

Intersections in First
Quadrant for ASME-

Elliptic and Langer
Failure Criteria

Intersecting Equations	Intersection Coordinates
$\left(\frac{S_a}{S_e}\right)^2 + \left(\frac{S_m}{S_y}\right)^2 = 1$ Load line $r = S_a/S_m$	$S_a = \sqrt{\frac{r^2 S_e^2 S_y^2}{S_e^2 + r^2 S_y^2}}$ $S_m = \frac{S_a}{r}$
$\frac{S_a}{S_y} + \frac{S_m}{S_y} = 1$ Load line $r = S_a/S_m$	$S_a = \frac{r S_y}{1 + r}$ $S_m = \frac{S_y}{1 + r}$
$\left(\frac{S_a}{S_e}\right)^2 + \left(\frac{S_m}{S_y}\right)^2 = 1$ $\frac{S_a}{S_y} + \frac{S_m}{S_y} = 1$	$S_a = 0, \frac{2 S_y S_e^2}{S_e^2 + S_y^2}$ $S_m = S_y - S_a, r_{\text{crit}} = S_a/S_m$

Fatigue factor of safety

$$n_f = \sqrt{\frac{1}{(\sigma_a/S_e)^2 + (\sigma_m/S_y)^2}}$$

Torsional Fatigue Strength under Fluctuating Stresses

In constructing the Goodman diagram:

$$S_{su} = 0.67S_{ut}$$

Also, from distortion-energy theory

$$S_{sy} = 0.577S_{yt}$$

Combinations of Loading Modes

It may be helpful to think of fatigue problems as being in three categories:

- Completely reversing simple loads
- Fluctuating simple loads
- *Combinations of loading modes*

$$\sigma' = (\sigma_x^2 + 3\tau_{xy}^2)^{1/2}$$

$$\sigma'_a = \left\{ \left[(K_f)_{\text{bending}}(\sigma_a)_{\text{bending}} + (K_f)_{\text{axial}} \frac{(\sigma_a)_{\text{axial}}}{0.85} \right]^2 + 3 \left[(K_{fs})_{\text{torsion}}(\tau_a)_{\text{torsion}} \right]^2 \right\}^{1/2}$$

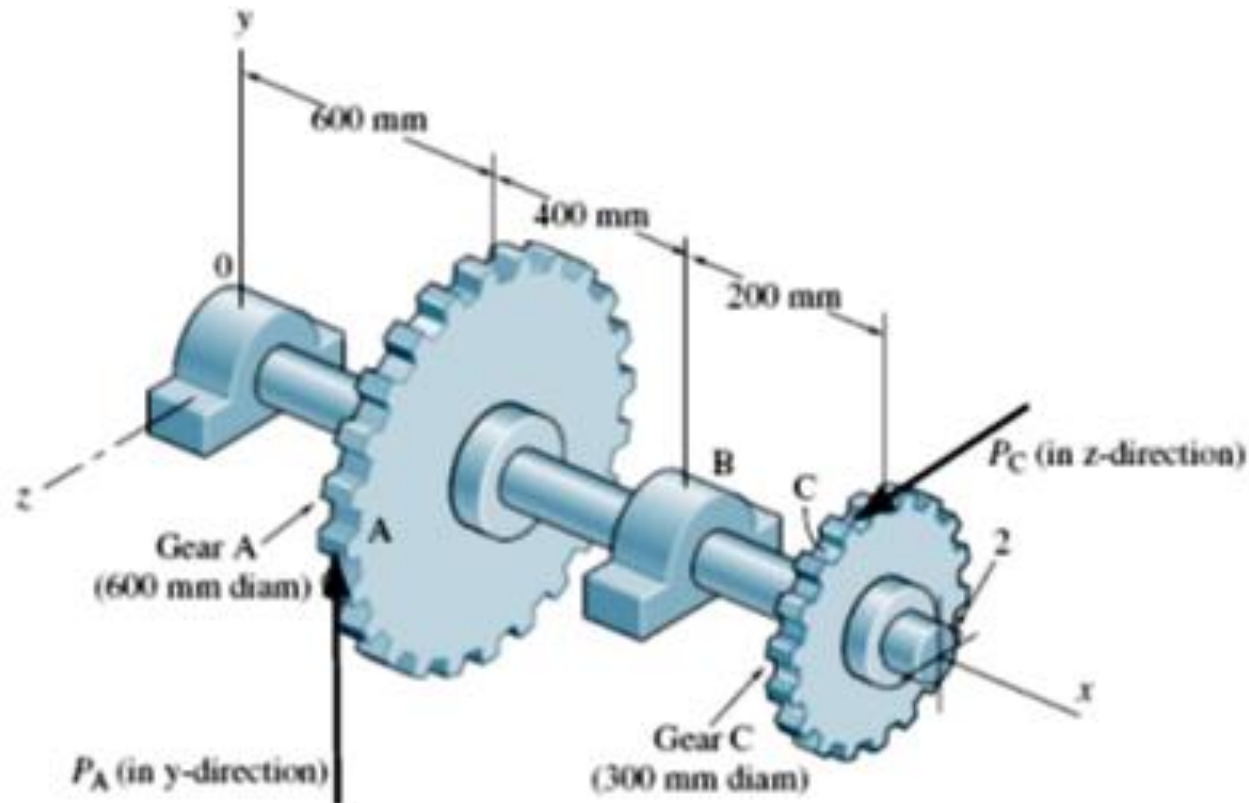
$$\sigma'_m = \left\{ \left[(K_f)_{\text{bending}}(\sigma_m)_{\text{bending}} + (K_f)_{\text{axial}}(\sigma_m)_{\text{axial}} \right]^2 + 3 \left[(K_{fs})_{\text{torsion}}(\tau_m)_{\text{torsion}} \right]^2 \right\}^{1/2}$$

Examples

The shaft shown supports two gears. The shaft is made from high carbon steel (AISI 1080, HR), and is to be designed with a safety factor of 2.0. The gears transmit a constant torque caused by $P_A = 2000 \text{ N}$ acting vertically as shown.

The shaft has a constant machined cross-section. ($S_y = 420 \text{ MPa}$, $S_{ut} = 770 \text{ MPa}$)

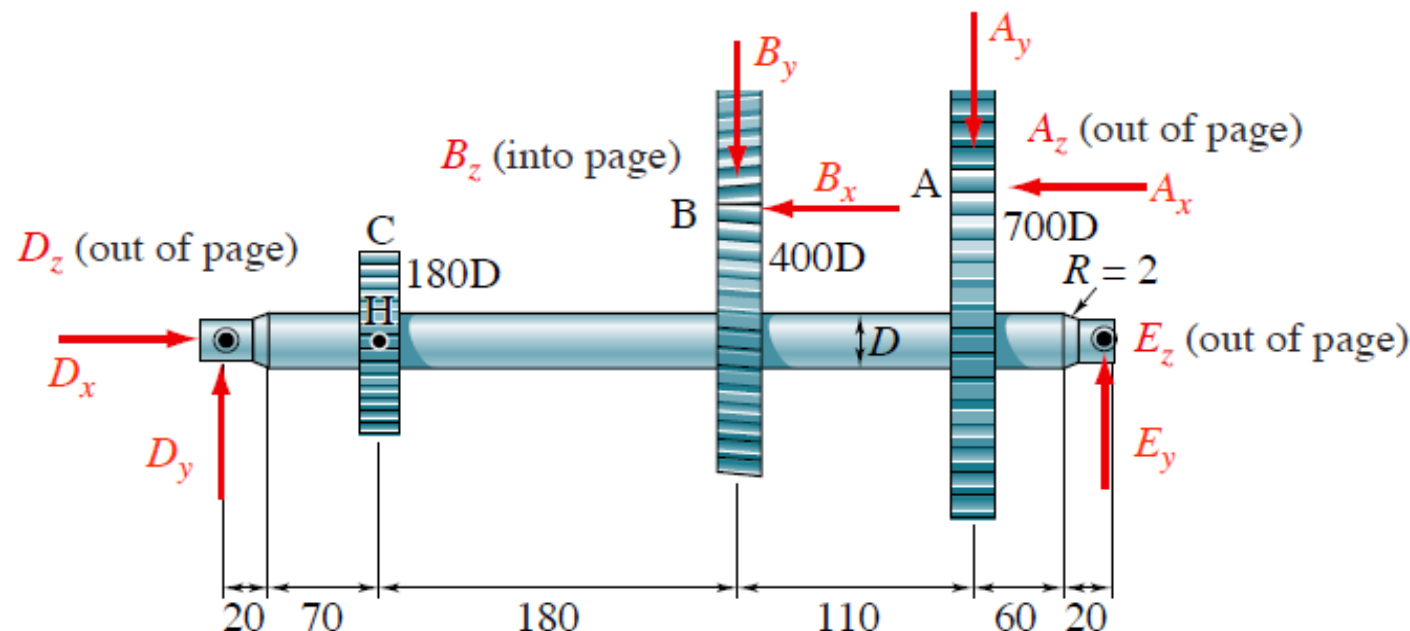
- What is the reaction force on gear C?
- Using the Soderberg line, obtain the required shaft diameter



Examples

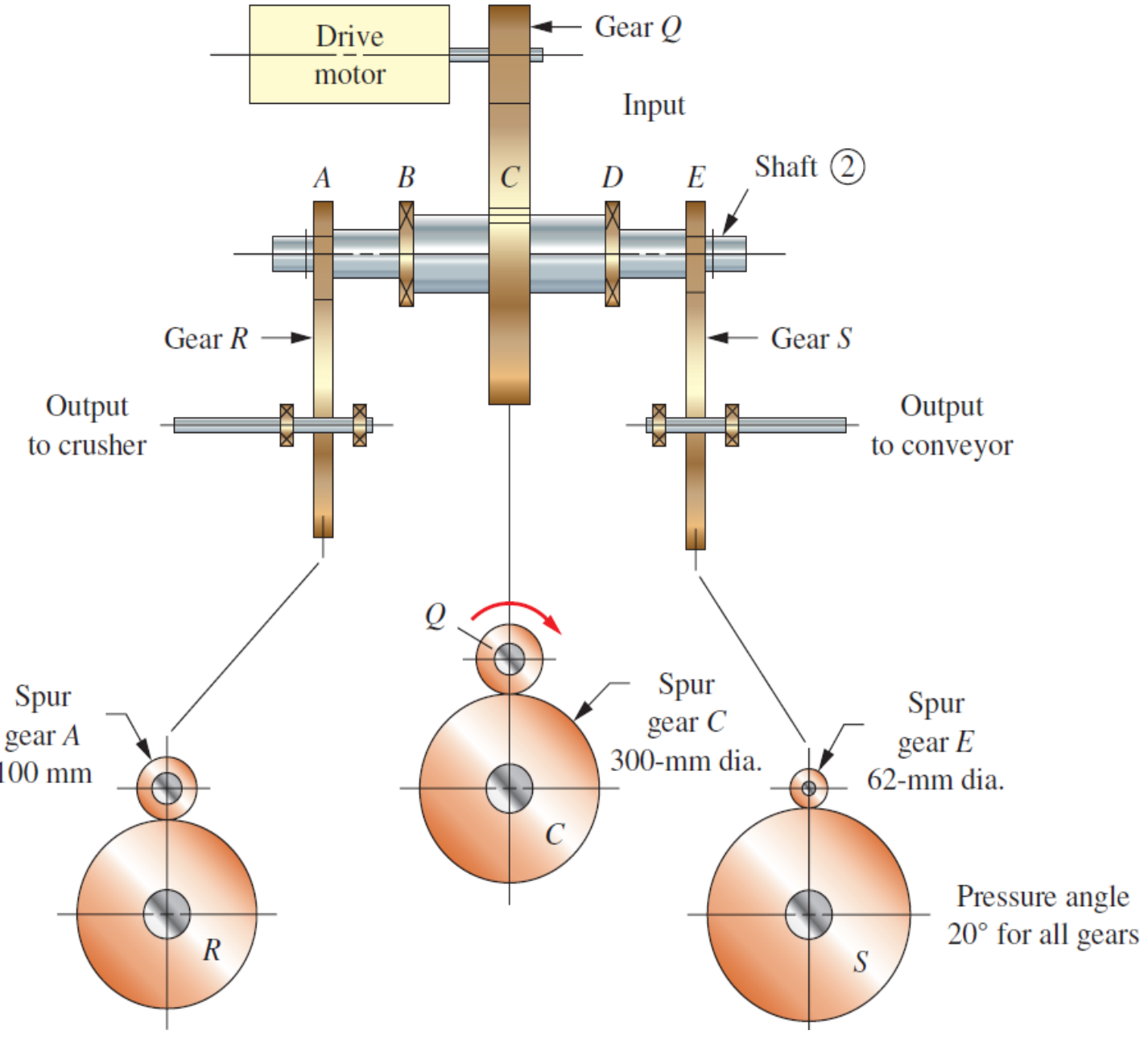
The shaft shown rotates at 1000 rpm and transfers 6 kW of power from input gear A to output gears B and C. All important surfaces are ground. All dimensions in mm. The shaft is made of annealed carbon steel with $S_{ut} = 636 \text{ MPa}$ and $S_y = 365 \text{ MPa}$.

- Draw a free-body diagram as well as the shear and moment diagrams of the shaft.
- Determine the minimum shaft diameter for a safety factor of 2 and 99% reliability.



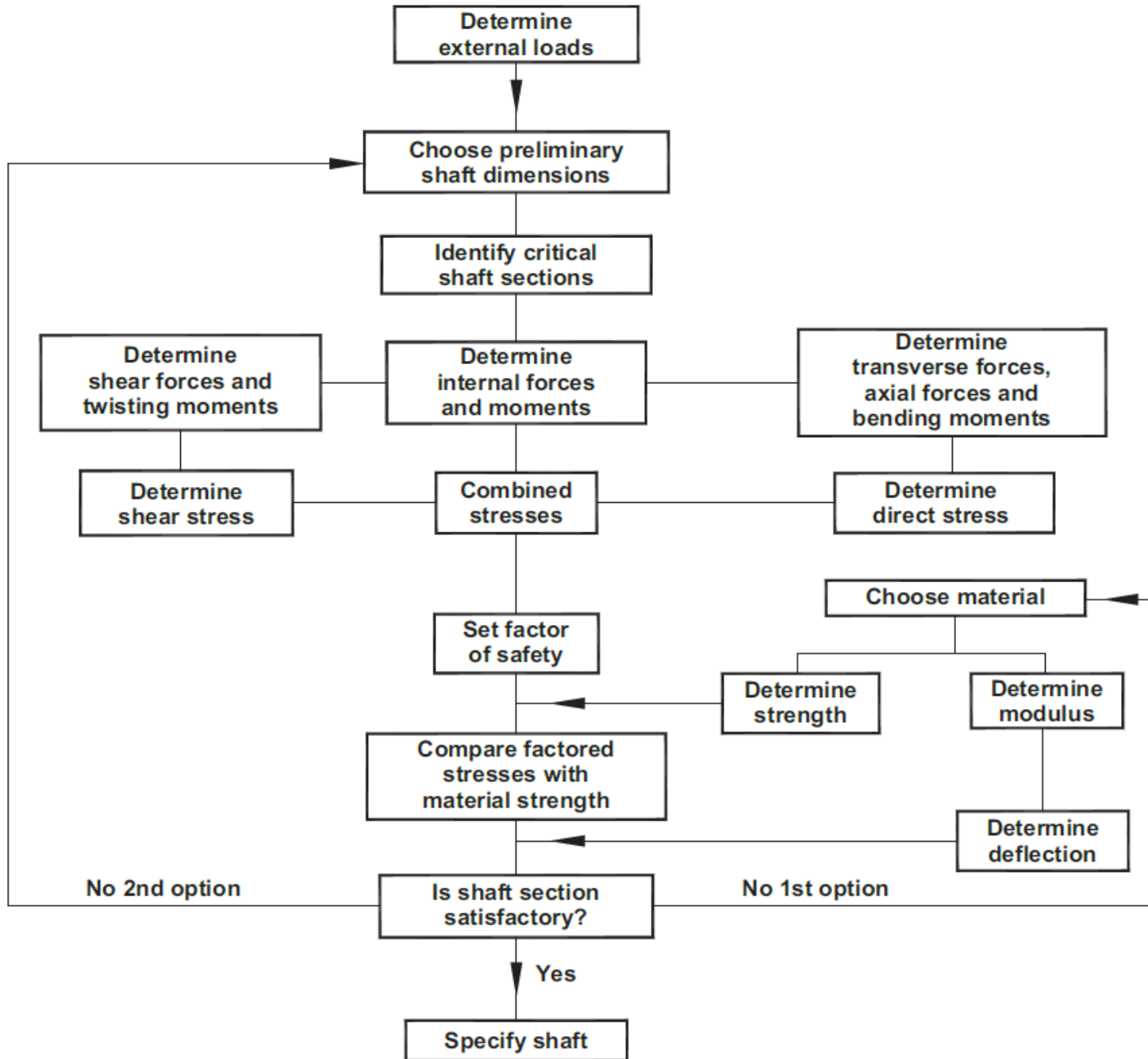
Mini Project

A drive for a system to crush coal and deliver it by conveyor to a railroad car is shown below. Gear A delivers 15 kW to the crusher and gear E delivers 7.5 kW to the conveyor. All power enters the shaft through gear C. The shaft carrying gears A, C, and E rotates at 480 rpm. Design that shaft. The distance from the middle of each bearing to the middle of the face of the nearest gear is 100 mm. Make appropriate assumptions where necessary. Justify all assumptions.



Mini Project

Design procedure flow chart for shaft strength and rigidity. (Mechanical Design Engineering Handbook, Peter R.N. Childs, 2014)



Mini Project

